Available online at www.sciencedirect.com
SCIENCE DIRECT®
Journal of Sound and Vibration 282 (2005) 679–700
JOURNAL OF SOUND AND VIBRATION
www.elsevier.com/locate/jsvi

An energy finite element formulation for high-frequency vibration analysis of externally fluid-loaded cylindrical shells with periodic circumferential stiffeners subjected to axi-symmetric excitation

Weiguo Zhang[a], Nickolas Vlahopoulos[b,*], Kuangcheng Wu[c]

[a]*Department of Naval Architecture and Marine Engineering, University of Michigan, Ann Arbor, MI 48109-2145, USA*
[b]*Department of Naval Architecture and Marine Engineering/Mechanical Engineering, University of Michigan, Ann Arbor, MI 48109-2145, USA*
[c]*Signatures and Hydrodynamics, Northrop Grumman Newport News, Newport News, VA 23607-2770, USA*

Received 21 April 2003; accepted 3 March 2004

Abstract

A hybrid method is developed for predicting the high-frequency vibration response of fluid-loaded cylindrical shells with periodic circumferential stiffeners. In this method, the cylindrical shell is modeled using the Energy Finite Element Analysis (EFEA) method which includes added mass and radiation effects due to the surrounding exterior fluid medium. The joint matrices of the EFEA formulation at the location of the periodic stiffeners are computed based on Periodic Structure (PS) theory. Thus, the periodicity effects such as pass/stop characteristics are captured in the EFEA solution. The hybrid EFEA-PS method is used to analyze the vibration of a fluid-loaded axisymmetric cylindrical shell with periodic circumferential stiffeners. The flexural energy stored in each periodic section is computed. The results are compared with the solution produced by a very dense axisymmetric Finite Element (FE) model with infinite finite elements for the fluid domain. The good correlation indicates that the new hybrid method captures properly both the heavy fluid effects of the exterior fluid medium and the periodicity characteristics due to periodic stiffeners.

*Corresponding author. Tel.: +1-734-764-8341; fax: +1-734-936-8820.
E-mail address: nickvl@engin.umich.edu (N. Vlahopoulos).

0022-460X/$ - see front matter © 2004 Elsevier Ltd. All rights reserved.
doi:10.1016/j.jsv.2004.03.063

1. Introduction

The objective of this paper is to present the formulation and the validation of an Energy Finite Element Analysis (EFEA) formulation that can model the high-frequency vibration of cylindrical shells with periodic circumferential stiffeners under external heavy fluid loading. Recently, an EFEA method for computing high-frequency vibration of structures either in vacuum or in contact with a dense fluid has been presented [1–3]. The presence of heavy fluid loading has been considered through added mass and radiation damping. The presence of discontinuities due to stiffeners was also incorporated in the derivation of the EFEA formulation. The EFEA developments were validated by comparing EFEA results to solutions obtained by very dense conventional finite element models and solutions from classical techniques such as the Statistical Energy Analysis (SEA) method and the modal decomposition method for bodies of revolution [1–3]. However, the periodicity effects that are encountered in cylindrical shells with circumferential stiffeners have not been accounted in the existing EFEA formulations. Specifically, the distinctive vibrational characteristics associated with the pass/stop bands frequency intervals of a periodically stiffened cylinder [4,5] are not captured. In this paper, a hybrid method which combines the EFEA method with Periodic Structure (PS) theory is developed for analyzing the vibration response of fluid-loaded cylindrical shells with periodic circumferential stiffeners subjected to high-frequency circumferential excitations.

The SEA method is a mature and established analysis technique for high-frequency vibrations [6,7]. Efforts in including the effect of periodic stiffeners in SEA are reviewed first. In SEA, a vibro-acoustic system is divided into subsystems of similar modes. The lumped averaged energy within each subsystem of similar modes comprises the primary SEA variable and the power transferred between subsystems is expressed in terms of coupling loss factors. Crighton [8] suggested that the resonance frequencies and mode shapes that included the effect of fluid loading can be utilized in defining the dynamics of the corresponding subsystems when predicting the dynamic response of plates under fluid loading in SEA. A method was proposed by Keane et al. [9] to construct an enhanced probabilistic model for modeling periodic structures in SEA. The model was based on calculating the pass bands of typical elements of the periodic structure, thus allowing SEA to reflect the highly non-uniform distribution of natural frequencies found in the periodic structures. Langley et al. [10] studied the high-frequency vibration transmission through a periodically stiffened panel within the context of SEA. The periodically stiffened panel was modeled as a damped coupled element between adjoining structural components and the transmission and absorption coefficients were calculated on the basis of periodic structure theory. Langley [11] also presented a derivation for a wide band frequency averaged power transmission coefficient of a one-dimensional periodic system. When the wide band excitation was considered to cover both pass bands and stop bands, the averaged power transmission coefficients included the periodicity characteristics of the structure. Heavy fluid loading effects were not accounted in any of the previous SEA formulations for periodic structures.

As an alternative formulation to the SEA method, the Energy Finite Element Analysis (EFEA) method is a recently developed analytical tool for high-frequency structural/acoustic simulations [1–3,12–16]. The primary variable in EFEA is defined as the time averaged over a period and space averaged over a wavelength energy density (energy density). The governing differential equations are developed with respect to the energy density, and a finite element approach is

employed for the numerical solution. A joint matrix computed from the power transmission coefficients is utilized for coupling the energy density variables across any discontinuities, such as change of plate thickness, plate/stiffener junctions, etc. The EFEA exhibits some unique features for a high-frequency method, such as generation of the numerical model based on geometry, damping treatment can be applied locally and it can vary with respect to location. Results for the energy density are computed separately for each location and spatial presentation of the result is possible. Nevertheless, the current EFEA formulation does not capture any behavior associated with a periodically stiffened structure. When considering the high-frequency vibration of a plate under fluid loading, the flexural wavelength is smaller than the interval length between two periodic stiffeners, therefore the stiffener stiffness cannot be smeared by computing an equivalent rigidity for the plate [10]. The periodic stiffeners must be regarded as coupling components between periodic units. In this formulation, PS theory is utilized for computing the coupling joint matrix and for accounting for the periodicity characteristics.

A structure is considered as a periodic structure when it is composed by a number of identical units connected in a regular pattern. A cylindrical shell with periodic circumferential stiffeners and subjected to external fluid loading is considered in the present work. The cylindrical shell forms a periodic structure with a basic unit consisting of a single bay of the cylindrical shell with a circumferential stiffener at each end. A periodic structure possess the property of having some frequency bands (pass bands) in which free wave propagation is possible and other bands (stop bands) in which it is impossible. SenGupta [4] presented an overview of application of periodic structure theory in the analysis of dynamic responses of periodic structures. For a flexural wave traveling from one periodic unit to the next, the amplitudes of two points at adjacent units which are separated by the periodic distance are related by propagation constants. The propagation constants may be real, purely imaginary or generally complex. The pass bands or stop bands are determined by the propagation constants. Mead [5] outlined systemically methods for analyzing and for predicting the free and forced wave motion in continuous and periodic structures. A formulation for computing the propagation constants of a cylindrical shell with periodic axial stiffeners or circumferential stiffeners is presented by Mead and Bardell in Refs. [17,18], respectively. The decay of the amplitude of the flexural vibration from one periodic unit to the next is determined by the attenuation constants which are defined as the real part of the propagation constants. Thus, the energy ratio between energy stored in two adjacent periodic units can be computed from the attenuation constants. The energy ratio is employed for computing the EFEA power transfer coefficients.

A hybrid method combining PS theory with the EFEA is presented in this paper. In this method, all periodic units are modeled using the EFEA method which incorporates the added mass and radiation effects due to heavy fluid [2]. The joint matrices of the EFEA formulation at stiffeners' locations are calculated from the energy ratio between two adjacent periodic units based on the following procedure. The propagation constants for a cylindrical shell with periodic circumferential stiffeners subjected to external fluid loading are evaluated from a formulation which is based on Ref. [18] but modified to include the added mass effect due to the fluid loading. The flexural energy ratio between two adjacent periodic units is evaluated from the attenuation constants which correspond to the flexural wave type. An algorithm from Ref. [19] is employed for deriving the power transfer coefficients from the energy ratio between two adjacent periodic units. The power transfer coefficients account for the periodicity characteristics and are utilized in

computing the joint matrices of the EFEA formulation. The energy density distribution over the entire periodic structure is computed by the EFEA model which includes the periodicity effects through the formulation of the joint matrices.

In order to validate the new development, the vibration of a cylindrical shell with periodically circumferential stiffeners and subjected to circumferential excitation is analyzed. Similar type of axisymmetric structures have been studied by others. For example, Beskos [20] presented a numerical method for computing the low-frequency vibration of a stiffened cylindrical shell. Using theoretical methods, Photiadis [21] examined the response of a periodically ribbed fluid-loaded cylindrical shell with focus on the effects due to mixing of the different wave types. In this paper, the vibration of a periodically stiffened cylinder subjected to an external ring force is computed by the hybrid EFEA-PS method. The same structure is analyzed by a validated axisymmetric finite element code (SONAX [22]). In SONAX, the cylindrical shell and the periodic stiffeners are modeled with very dense structural finite elements in order to capture the short wavelength response at high frequencies. The exterior fluid medium is modeled with finite fluid elements and with infinite fluid elements. In the past it has been demonstrated that FE techniques can calculate accurately the behavior of periodic structures [23] and the fluid–structural interaction [24]. The computations are performed at the frequency ranges where both the EFEA-PS and the FEA method are valid. The energy ratios between the energy stored in receiving periodic units and the excited unit are computed by the two methods and compared. The frequency range where analyses are performed are well below the coincidence frequency and much higher than the ring frequency of the cylindrical shell.

2. Overview of EFEA formulation for a plate structures under fluid loading

The EFEA formulation for plate structures in contact with heavy fluid on one side is overviewed in this Section [2]. The EFEA formulation is developed by considering the flexural displacement of a plate as a linear superposition of incoherent waves associated with any two orthogonal directions x and y [1]:

$$w_x = (A_x e^{-i\gamma_x x} + B_x e^{i\gamma_x x}) e^{i\omega t}, \quad w_y = (A_y e^{-i\gamma_y y} + B_y e^{i\gamma_y y}) e^{i\omega t}, \tag{1}$$

where A_x, A_y, B_x, B_y are constants associated with the waves in x and y directions, γ_x and γ_y are the corresponding complex flexural wavenumbers of the fluid-loaded plate. The flexural wavenumbers are defined as [2]

$$\gamma_x = \gamma_{x1}\left(1 - i\frac{\eta}{4}\right), \quad \gamma_y = \gamma_{y1}\left(1 - i\frac{\eta}{4}\right), \tag{2}$$

where

$$\gamma_{x1} = \gamma_{y1} = \sqrt[4]{\frac{m_{\text{eff}}}{D}\,\omega^2}, \quad \eta = \eta_{\text{damp}} + \eta_{\text{rad}}. \tag{3}$$

The effective mass m_{eff} and the radiation damping η_{rad} are evaluated:

$$m_{\text{eff}} = \begin{cases} m\left(1 + \dfrac{\rho}{m\sqrt{k_f^2 - k^2}}\right), & f \leqslant f_C, \\ m, & f > f_C; \end{cases} \quad \eta_{\text{rad}} = \begin{cases} \dfrac{\rho c}{\omega m_{\text{eff}}}\,\sigma_{\text{rad}}, & f \leqslant f_C, \\ \dfrac{\rho}{m\sqrt{k^2 - k_f^2}}, & f > f_C; \end{cases} \tag{4}$$

where D is the bending stiffness of the plate, $m = \rho_s h$ is the plate surface mass density, η_{damp} is the structural damping factor, η is the total damping factor, ρ is the mass density of the fluid, k_f is the flexural wavenumber of the plate in vacuum, k is the acoustical wavenumber of the fluid medium, σ_{rad} is the radiation efficiency considering edge and corner effect for a finite plate [25,26], and f_C is the coincidence frequency. Subscript "eff " indicates the added mass effect.

An expression for the energy density and the intensity is derived for each one of the two orthogonal waves. By neglecting higher-order damping terms, the time and space averaged energy density and intensity become

$$\langle \underline{e}_x \rangle = \frac{D}{4}\left[\left(\gamma_{x1}^4 + \frac{m_{\text{eff}}}{D}\,\omega^2\right)\left(A_x^2 \mathrm{e}^{-(\eta/2)\gamma_{x1}x} + B_x^2 \mathrm{e}^{(\eta/2)\gamma_{x1}x}\right)\right], \tag{5}$$

$$\langle \underline{I}_x \rangle = D\gamma_{x1}^3 \omega\left(A_x^2 \mathrm{e}^{-(\eta/2)\gamma_{x1}x} - B_x^2 \mathrm{e}^{(\eta/2)\gamma_{x1}x}\right), \tag{6}$$

$$\langle \underline{e}_y \rangle = \frac{D}{4}\left[\left(\gamma_{y1}^4 + \frac{m_{\text{eff}}}{D}\,\omega^2\right)\left(A_y^2 \mathrm{e}^{-(\eta/2)\gamma_{y1}y} + B_y^2 \mathrm{e}^{(\eta/2)\gamma_{y1}y}\right)\right], \tag{7}$$

$$\langle \underline{I}_y \rangle = D\gamma_{y1}^3 \omega\left(A_y^2 \mathrm{e}^{-(\eta/2)\gamma_{y1}y} - B_y^2 \mathrm{e}^{(\eta/2)\gamma_{y1}y}\right). \tag{8}$$

The averaged energy density and intensity of the flexural waves constitute the primary energy variables of the EFEA formulation. The vibration of the plate is considered as incoherent since at high frequencies the flexural wavelength is small compared to the dimension of the plate and the multiple reflections from the boundaries create an incoherent field. This assumption is equivalent to the SEA assumption of considering the energy stored in a group of similar modes as a summation of the energy stored in each individual mode. Therefore, the total energy density and the total intensity at a point are derived as the summation of the energy variables associated with each one of the members of the orthogonal basis that represents the vibration:

$$\langle \underline{e} \rangle = \langle \underline{e}_x \rangle + \langle \underline{e}_y \rangle = \frac{D}{2}\left[\gamma_{x1}^4\left(A_x^2 \mathrm{e}^{-(\eta/2)\gamma_{x1}x} + B_x^2 \mathrm{e}^{(\eta/2)\gamma_{x1}x}\right) + \gamma_{y1}^4\left(A_y^2 \mathrm{e}^{-(\eta/2)y_{y1}y} + B_y^2 \mathrm{e}^{(\eta/2)y_{y1}y}\right)\right], \tag{9}$$

$$\langle \underline{\mathbf{I}} \rangle = \langle \underline{I}_x \rangle \mathbf{i} + \langle \underline{I}_y \rangle \mathbf{j} = D\omega\left[\gamma_{x1}^3\left(A_x^2 \mathrm{e}^{-(\eta/2)\gamma_{x1}x} - B_x^2 \mathrm{e}^{(\eta/2)\gamma_{x1}x}\right)\mathbf{i} + \gamma_{y1}^3\left(A_y^2 \mathrm{e}^{-(\eta/2)\gamma_{y1}y} - B_y^2 \mathrm{e}^{(\eta/2)\gamma_{y1}y}\right)\mathbf{j}\right]. \tag{10}$$

By observing the similarities between Eqs. (11) and (12), a relationship between the energy density and the intensity is derived:

$$\langle \underline{\mathbf{I}} \rangle = -\frac{(c_g)_{\text{eff}}^2}{\eta\omega}\,\nabla\langle \underline{e} \rangle, \tag{11}$$

where $(c_g)_{\text{eff}} = 2 * \sqrt[4]{(D/m_{\text{eff}})\omega^2}$, is defined as the effective group velocity for the fluid-loaded plate. The EFEA governing differential equation for a fluid-loaded plate is derived by considering a power balance at the steady state over a differential control volume of the plate [27], the relationship between dissipated power and energy stored on the plate and the relationship between energy density and intensity (Eq. (11)):

$$-\frac{(c_g)_{\text{eff}}^2}{\eta\omega}\nabla^2\langle \underline{e}\rangle + \eta\omega\langle \underline{e}\rangle = \langle \underline{\Pi}_{\text{in}}\rangle. \tag{12}$$

A finite element formulation is employed for solving Eq. (12) numerically. The element level system of equations are

$$[E^e_{\text{eff}}]\{e^e\} = \{F^e\} + \{Q^e\}, \tag{13}$$

where superscript e indicate element-based quantities, $\{e^e\}$ is the vector of nodal values of the energy density at the nodes of a finite element, $[E^e_{\text{eff}}]$ is the effective system matrix for the element which includes the heavy fluid effect, $\{F^e\}$ is the vector of external input power at the nodal locations of the element, and $\{Q^e\}$ is the vector of the internal power flow across the element boundary which provides the mechanism for assembling the global system of equations for adjacent elements and for connecting elements across discontinuities. At the boundaries of the plates between discontinuities, the energy density is discontinuous and the coupling in the global system of equations is achieved by accounting for continuity in the power flow. The vector of internal power flow $\{Q\}$ is expressed as a product between the joint matrix and the nodal values of the energy density. The joint matrix represents the power transmission mechanism across the discontinuity:

$$\begin{Bmatrix} Q^i_n \\ Q^i_{n+1} \\ Q^j_m \\ Q^j_{m+1} \end{Bmatrix} = [J_{\text{eff}}]^i_j \begin{Bmatrix} e^i_n \\ e^i_{n+1} \\ e^j_m \\ e^j_{m+1} \end{Bmatrix}, \tag{14}$$

where i and j refer to the two elements connected at the discontinuity, n and $n+1$ indicate the two nodes of the i element at the joint, m and $m+1$ indicate the two nodes of the j element at the joint, $[J_{\text{eff}}]^i_j$ is the joint matrix which captures the mechanism of power transfer between elements i and j across the discontinuity. In this paper, the joint matrix is computed based on PS theory and accounts for the heavy fluid loading effect. Introducing Eq. (14) into Eq. (13) results in

$$\left(\begin{bmatrix} [E^e_{\text{eff}}]_i & \\ & [E^e_{\text{eff}}]_j \end{bmatrix} + [JC_{\text{eff}}]^i_j \right) \begin{Bmatrix} \{e^i\} \\ \{e^j\} \end{Bmatrix} = \begin{Bmatrix} \{F^e\}_i \\ \{F^e\}_j \end{Bmatrix}, \tag{15}$$

where $[E^e_{\text{eff}}]_i$, $[E^e_{\text{eff}}]_j$ are the element matrices for the ith and jth element, $\{e^i\}$, $\{e^j\}$ are vectors containing all the nodal degrees of freedom for element i and j, respectively. $[JC_{\text{eff}}]^i_j$ is a coupling matrix comprised by the coefficients of $[J_{\text{eff}}]^i_j$ positioned in the appropriate locations. The assembly of the element matrices between elements with no discontinuities is performed in the conventional finite element manner without any coupling matrices since in this case, the energy

density is continuous at the nodes between elements. The final system of EFEA equations is

$$\left[[E_{\text{eff}}] + \sum [JC_{\text{eff}}]\right]\{\langle \underline{e} \rangle\} = \{f\}, \tag{16}$$

where $\sum$ indicates the summation of all the coupling matrices that correspond to all the discontinuities in the model.

3. Derivation of joint matrix for a periodic stiffener from periodic structure theory

The power transfer coefficients at the locations of the periodic stiffeners are derived based on PS theory. The derivation is performed by considering axisymmetric excitation only, therefore only axisymmetric wave motion need to be considered in the cylindrical shell. The wave solution for the axisymmetric vibration in a periodically stiffened cylindrical shell under external fluid loading is presented first, and the associated propagation constants are derived. The propagation constants are employed for determining appropriate values for the power transfer coefficients between adjacent periodic units at the locations of the stiffeners. Thus, the joint matrices of the EFEA formulation corresponding to the periodic stiffeners include the periodic effects.

3.1. Wave solution for the axisymmetric vibration of a cylindrical shell subjected to external fluid loading

The equations of motion for the axisymmetric vibration of an externally fluid-loaded cylindrical shell (Fig. 1(a)) are [28]

$$\frac{E_c h}{(1-v^2)}\frac{\partial^2 u}{\partial x^2} - \rho_s h \frac{\partial^2 u}{\partial t^2} + \frac{E_c h v}{(1-v^2)R}\frac{\partial w}{\partial x} = 0, \tag{17}$$

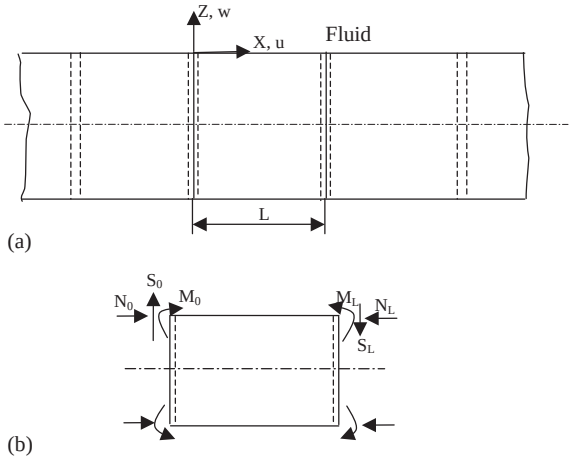

Fig. 1. (a) A periodic ring stiffened cylindrical shell immersed into a dense fluid and the corresponding coordinate system. (b) One periodic section (including one bay cylindrical shell and a half stiffener attached circumferentially at each end).

$$\frac{E_c h v}{(1-v^2)R}\frac{\partial u}{\partial x}+\frac{E_c h^3}{12(1-v^2)}\frac{\partial^4 w}{\partial x^4}+\frac{E_c h}{(1-v^2)R^2}w+\rho_s h\frac{\partial^2 w}{\partial t^2}=-p_{z=0}, \tag{18}$$

where $u(x,t)$, $w(x,t)$ are the longitudinal and flexural displacements of the cylindrical shell, respectively; R is the radius of the shell; E_c is the complex modulus of elasticity which is of the form $E(1+\mathrm{i}\eta)$; η is the total damping factor defined in Section 2; ρ_s is the mass density of the shell; v is the Poisson ratio; h is the shell thickness; and $p_{z=0}$ is the pressure exerted by the external fluid on the vibrating shell.

The wave solutions for the displacements are [18]

$$u=\sum_{s=1}^{6}A_s e^{\lambda_s x}e^{\mathrm{i}\omega t},\quad w=\sum_{s=1}^{6}C_s e^{\lambda_s x}e^{\mathrm{i}\omega t}, \tag{19,20}$$

where λ_s, $s=1,\ldots,6$, are the eigenvalues of the characteristic equation for the determinant of Eqs. (17) and (18):

$$\begin{vmatrix} 2\lambda_s^2+\dfrac{2\rho_s(1-v^2)}{E_c}\omega^2 & \dfrac{2v}{R}\lambda_s \\ \dfrac{2v}{R}\lambda_s & \dfrac{2}{R^2}+\dfrac{h^2}{6}\lambda_s^4-\dfrac{2(\rho_s)_{\mathrm{eff}}(1-v^2)}{E_c}\omega^2 \end{vmatrix}=0. \tag{21}$$

The effective mass density $(\rho_s)_{\mathrm{eff}}$ is introduced in the equations due to the fluid loading effect. Since at high frequencies the general effect of the fluid loading on a cylindrical shell is similar to the fluid loading effect on a plate [29] and since the dispersion relation for a particular wave guide, such as the axisymmetric wave, of a cylindrical shell is nearly coinciding with planar solutions at frequencies higher than the ring frequency [29], the effective mass density of a flat plate under fluid loading is utilized in Eq. (21):

$$(\rho_s)_{\mathrm{eff}}=\rho_s\left(1+\frac{\rho}{\rho_s h\sqrt{k_f^2-k^2}}\right), \tag{22}$$

where k_f is the flexural wave number of the plate in vacuum, ρ is the fluid mass density, and k is the acoustic wavenumber in the fluid medium.

For each eigenvalue λ_s of Eq. (21), a relationship between the corresponding wave amplitudes A_s and C_s is established from the characteristic equations:

$$\begin{bmatrix} B_{11}(\lambda_s) & B_{12}(\lambda_s) \\ B_{21}(\lambda_s) & B_{22}(\lambda_s) \end{bmatrix}\begin{Bmatrix} A_s \\ C_s \end{Bmatrix}=\begin{Bmatrix} 0 \\ 0 \end{Bmatrix},\quad s=1,\ldots,6, \tag{23}$$

resulting in

$$A_s=-\frac{B_{12}(\lambda_s)}{B_{11}(\lambda_s)}C_s=\psi(\lambda_s)C_s. \tag{24}$$

The expressions of $B_{11}(\lambda_s), B_{12}(\lambda_s), B_{21}(\lambda_s), B_{22}(\lambda_s)$ are derived from Eq. (21). Thus, both displacements u and w can be expressed in terms of one set of wave amplitudes C_s based on Eqs. (19), (20), and (24).

3.2. Derivation of propagation constant from periodic structure theory

The edge displacements and force/moment resultants acting on the edges of a periodic section (Fig. 1(b)) are related by the equation [18]

$$\begin{Bmatrix} N \\ S \\ M \\ u \\ w \\ w' \end{Bmatrix}_{x=L} = \mathrm{e}^{\mu} \begin{Bmatrix} -N \\ -S \\ -M \\ u \\ w \\ w' \end{Bmatrix}_{x=0} \tag{25}$$

where μ is defined as a propagation constant. The force and moment resultants along the two circumferential stiffened edges can be expressed in terms of the displacement fields u and w and include the contribution from both the shell and the half stiffener. The corresponding expressions are [18]

$$N = \frac{E_c h}{(1-\nu^2)}\left(\frac{\partial u}{\partial x} + \frac{\nu}{R}\, w\right) + \tfrac{1}{2}\rho_0 A\left(\frac{\partial^2 u}{\partial t^2} - b\,\frac{\partial^3 w}{\partial x \partial t^2}\right), \tag{26}$$

$$S = -\frac{E_c h^3}{12(1-\nu^2)}\,\frac{\partial^3 w}{\partial x^3} + \frac{1}{2}\left(\frac{E_0 A}{R^2}\, w + \rho_0 A\,\frac{\partial^2 w}{\partial t^2}\right), \tag{27}$$

$$M = \frac{E_c h^3}{12(1-\nu^2)}\frac{\partial^2 w}{\partial x^2} + \frac{1}{2}\left(-\frac{E_0 I_{zz}}{R^2}\frac{\partial w}{\partial x} - \rho_0 I_p \frac{\partial^3 w}{\partial x \partial t^2} - \rho_0 A b \frac{\partial^2 u}{\partial t^2}\right), \tag{28}$$

where A is the cross-section area of the stiffener, ρ_0 is the stiffener mass density, E_0 is the modulus of elasticity of the stiffener, I_{zz} is the moment of inertia of the stiffener, I_p is the polar moment of inertia of the stiffener, and b is the eccentricity of the stiffener. In Eqs. (26)–(28), the contribution of the shell term at $x = 0$ is opposite in sign to that at $x = L$.

By substituting the displacement expressions from Eqs. (19), (20) and (24), and the force and moment expressions (26)–(28) into the periodic relationship provided by Eq. (25) results in

$$[K\_L]\{C_s\} = \mathrm{e}^{\mu}[K\_0]\{C_s\}, \tag{29}$$

where $[K\_0]$ is defined as a 6×6 structural property matrix of the periodic unit at $x = 0$ and is expressed as

$$[K\_0] = \begin{bmatrix} f_1(\lambda_1) & f_1(\lambda_2) & f_1(\lambda_3) & f_1(\lambda_4) & f_1(\lambda_5) & f_1(\lambda_6) \\ f_2(\lambda_1) & f_2(\lambda_2) & f_2(\lambda_3) & f_2(\lambda_4) & f_2(\lambda_5) & f_2(\lambda_6) \\ f_3(\lambda_1) & f_3(\lambda_2) & f_3(\lambda_3) & f_3(\lambda_4) & f_3(\lambda_5) & f_3(\lambda_6) \\ \psi(\lambda_1) & \psi(\lambda_2) & \psi(\lambda_3) & \psi(\lambda_4) & \psi(\lambda_5) & \psi(\lambda_6) \\ 1 & 1 & 1 & 1 & 1 & 1 \\ \lambda_1 & \lambda_2 & \lambda_3 & \lambda_4 & \lambda_5 & \lambda_6 \end{bmatrix}, \tag{30}$$

and $[K\_L]$ is defined as a 6×6 structural property matrix of the periodic unit at $x = L$ and is expressed as

$$[K\_L] = \begin{bmatrix} g_1(\lambda_1)e^{\lambda_1 L} & g_1(\lambda_2)e^{\lambda_2 L} & g_1(\lambda_3)e^{\lambda_3 L} & g_1(\lambda_4)e^{\lambda_4 L} & g_1(\lambda_5)e^{\lambda_5 L} & g_1(\lambda_6)e^{\lambda_6 L} \\ g_2(\lambda_1)e^{\lambda_1 L} & g_2(\lambda_2)e^{\lambda_2 L} & g_2(\lambda_3)e^{\lambda_3 L} & g_2(\lambda_4)e^{\lambda_4 L} & g_2(\lambda_5)e^{\lambda_5 L} & g_2(\lambda_6)e^{\lambda_6 L} \\ g_3(\lambda_1)e^{\lambda_1 L} & g_3(\lambda_2)e^{\lambda_2 L} & g_3(\lambda_3)e^{\lambda_3 L} & g_3(\lambda_4)e^{\lambda_4 L} & g_3(\lambda_5)e^{\lambda_5 L} & g_3(\lambda_6)e^{\lambda_6 L} \\ \psi(\lambda_1)e^{\lambda_1 L} & \psi(\lambda_2)e^{\lambda_2 L} & \psi(\lambda_3)e^{\lambda_3 L} & \psi(\lambda_4)e^{\lambda_4 L} & \psi(\lambda_5)e^{\lambda_5 L} & \psi(\lambda_6)e^{\lambda_6 L} \\ e^{\lambda_1 L} & e^{\lambda_2 L} & e^{\lambda_3 L} & e^{\lambda_4 L} & e^{\lambda_5 L} & e^{\lambda_6 L} \\ \lambda_1 e^{\lambda_1 L} & \lambda_2 e^{\lambda_2 L} & \lambda_3 e^{\lambda_3 L} & \lambda_4 e^{\lambda_4 L} & \lambda_5 e^{\lambda_5 L} & \lambda_6 e^{\lambda_6 L} \end{bmatrix}. \tag{31}$$

$\{C_s\}$ is the vector containing the amplitude coefficients of the flexural displacements,

$$\{C_s\} = \begin{Bmatrix} C_1 \\ C_2 \\ C_3 \\ C_4 \\ C_5 \\ C_6 \end{Bmatrix}. \tag{32}$$

The detail expressions of functions f_i and g_i are provided in Appendix A. The characteristic equation for computing the propagation constants is

$$[K]\{C_s\} = e^{\mu}\{C_s\}, \tag{33}$$

where $[K] = [K\_0]^{-1}[K\_L]$. The propagation constants μ are obtained from the eigenvalues e^{μ} of matrix $[K]$ [18].

Considering the amplitudes $|V_i(x)|$ and $|V_{i+1}(x)|$ of the velocity of the axisymmetric response along the length of two adjacent periodic units, respectively, the time averaged kinetic energy stored in the two periodic units are

$$\mathrm{KE}_i = \frac{1}{4}\left(\int_0^L \rho_s 2\pi Rh|V_i(x)|^2\,\mathrm{d}x\right), \quad \mathrm{KE}_{i+1} = \frac{1}{4}\left(\int_0^L \rho_s 2\pi Rh|V_{i+1}(x)|^2\,\mathrm{d}x\right). \tag{34,35}$$

The velocities at the two adjacent periodic units are related by the propagation constant $|V_{i+1}(x)| = e^{\mathrm{real}(\mu)}|V_i(x)|$. Therefore, the energy ratio between two adjacent units ($\mathrm{ER_{PS}}$) based on the periodic structure theory is computed as

$$\mathrm{ER_{PS}} = \frac{\mathrm{KE}_{i+1}}{\mathrm{KE}_i} = \frac{\int_0^L \rho_s 2\pi Rh(e^{\mathrm{real}(\mu)}|V_i(x)|)^2\,\mathrm{d}x}{\int_0^L \rho_s 2\pi Rh|V_i(x)|^2\,\mathrm{d}x} = (e^{\mathrm{real}(\mu)})^2. \tag{36}$$

The real part of the complex propagation constant comprises the attenuation constant.

The power transfer coefficients associated with the bending energy transmitted and reflected from the periodic stiffeners are evaluated from the energy ratio $\mathrm{ER_{PS}}$ computed by the periodic structure theory for two adjacent units. The attenuation constant corresponding to the flexural wave is employed for computing the energy ratio $\mathrm{ER_{PS}}$. An algorithm [19] developed in the past for computing the power transfer coefficients in EFEA applications from the energy ratio between

two adjacent components is also employed here in order to compute appropriate power transfer coefficients from the energy ratio evaluated by the periodic structure theory. According to the algorithm presented in Ref. [19], the EFEA model of the two adjacent components is utilized along with the known value of the energy ratio stored in the two components for computing the corresponding power transfer coefficients. An EFEA model comprised of two adjacent periodic cylindrical bays is constructed. One bay is defined as the excited section and the other comprises the receiving bay. The total energy stored at two bays is computed by the EFEA formulation while the EFEA system matrix is a function of the unknown power transfer coefficients. Then, the energy ratio between the two bays is defined as a function of the unknown power transfer coefficients. By accounting that the total power flow is constant, the two unknown power transfer coefficients are reduced to one unknown r:

$$\mathrm{ER}(r) = \frac{E(r)_{\mathrm{receivingbay}}}{E(r)_{\mathrm{excitedbay}}}. \tag{37}$$

An iterative algorithm [19] is employed for computing the power transfer coefficients based on the energy ratio of two adjacent units computed by the PS theory:

$$\frac{\mathrm{ER}(r)^{(n+1)} - \mathrm{ER}_{\mathrm{PS}}}{\mathrm{ER}(r)^{(n+1)} - \mathrm{ER}(r)^{(n)}} = \frac{r^{(n+1)} - r}{r^{(n+1)} - r^{(n)}}, \tag{38}$$

where superscript $n, (n+1)$ represent the consecutive iteration steps. The values of the power transfer coefficients computed by a diffuse wave assumption [30] are utilized in defining the initial value for coefficient r. The algorithm is considered to converge when the difference

$$\frac{\mathrm{ER}(r) - \mathrm{ER}_{\mathrm{PS}}}{\mathrm{ER}_{\mathrm{PS}}} < \mathrm{UL} \tag{39}$$

is smaller than a user-defined limit UL. The derived power transfer coefficients incorporate the periodic characteristics of the periodic circumferential stiffeners. The power transfer coefficients are utilized in the computation of the joint matrix [2,14]

$$[J_{\mathrm{eff}}]_j^i = ([I] - [\tau_{\mathrm{eff}}]_j^i)([I] + [\tau_{\mathrm{eff}}]_j^i)^{-1} \int_B \phi_i \phi_j \, \mathrm{d}B, \tag{40}$$

where ϕ_i, ϕ_j are Lagrangian basis functions, B is the boundary area between elements i and j at the joint, and $[\tau_{\mathrm{eff}}]_j^i$ is a matrix comprised by the power transfer coefficients. Since the joint matrices between all the elements at the periodic stiffeners contain the periodicity effects, the overall EFEA global system of equations which includes all the joint matrices also accounts for the periodic effects.

4. Validation

In order to validate the developed hybrid EFEA-Periodic Structure formulation (EFEA-PS), two different configurations of a fluid-loaded cylindrical shell with periodic stiffeners are analyzed. The radius of the cylindrical shell is 1.5 m and the distance between stiffeners in the two configurations is 0.38 and 1 m, respectively. Two different distances between stiffeners are utilized

in order to generate the stop bands at different frequency ranges in the two applications. The properties of the stiffeners are summarized in Table 1. The material properties for the structure and the surrounding fluid medium are listed in Tables 2 and 3. The EFEA model for the cylinder with 0.38 m distance between stiffeners is presented in Fig. 2. The model is comprised by 320 structural elements, 540 plate–plate joints, and 220 plate-periodic stiffener-plate joints. The results from the EFEA-PS analyses are compared to the solution computed by an established axisymmetric code with structural finite elements and acoustic infinite finite elements (SONAX [22]). In SONAX, the cylindrical shell and the periodic stiffeners are modeled with structural finite elements. The fluid medium is modeled with fluid finite elements and with infinite fluid finite elements. The fluid–structure interaction is accounted by the interface finite elements. The SONAX model includes 498 structural elements, 2331 finite fluid elements, 333 infinite fluid elements and 333 interface elements. The finite element mesh satisfies the condition that 10 elements are included in one wavelength of deformation at frequency up to 5000 Hz. The EFEA and the SONAX models for the cylinder with stiffeners placed 1 m apart are constructed in a similar manner. In order to process and compare the results, the cylindrical structures are divided into 10 periodic sections by 11 stiffeners (Fig. 2). The overall length of the two cylindrical structures differs between the two configurations since the number of periodic sections is the same but the distance between stiffeners differs. A circumferential excitation is applied at the left end of the cylindrical shell (periodic unit 1). Analyses are performed over the one-third octave bands between 2500 Hz and 5000 Hz. The analyzed frequencies are much above the ring frequency (around 540 Hz) and well below the coincidence frequency (around 18 000 Hz). In the frequency

Table 1
Cross-sectional properties of the stiffener and the cylinder

Stiffener	A (m^2)	1.1×10^{-3}
	I_{xx} (m^4)	6.06×10^{-6}
	I_{zz} (m^4)	2.867×10^{-7}
Cylinder	h (m)	1.27×10^{-2}

Table 2
Material properties of steel cylinder

Young's modulus (Pa)	2.07E + 11
Density (kg/m^3)	7800.0
Poisson's ratio	0.333
Damping loss factor	0.01
Longitudinal wave speed (m/s)	5464.0

Table 3
Properties of the fluid medium (water)

Density (kg/m^3)	1000.0
Sound speed (m/s)	1500.0

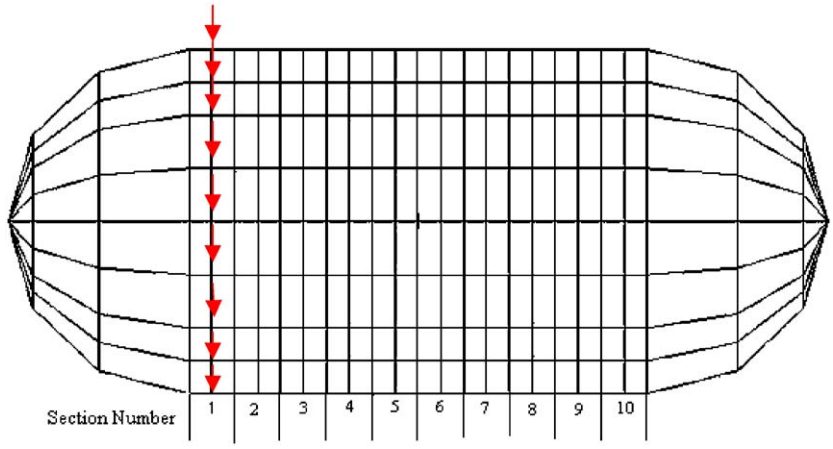

Fig. 2. EFEA model of the cylindrical shell and unit section division.

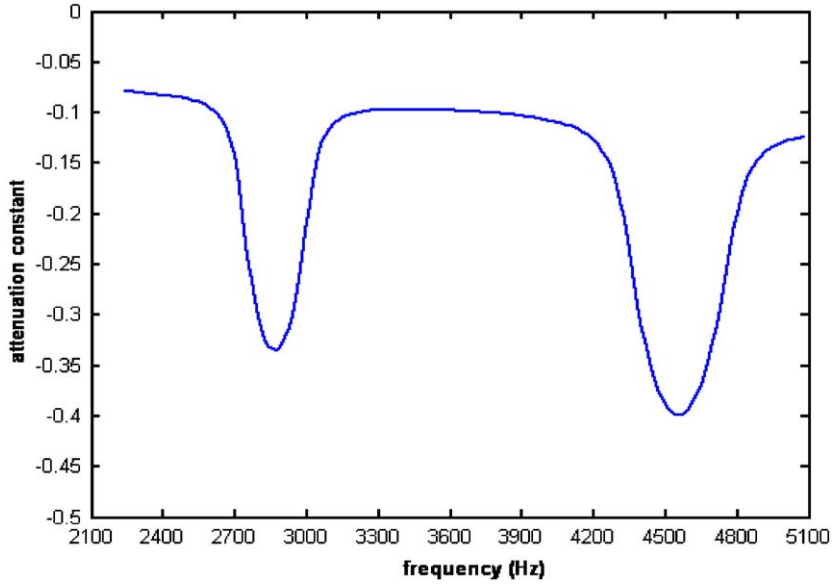

Fig. 3. The flexural wave attenuation constant of the circumferentially stiffened cylindrical shell with stiffeners spaced at 0.38 m.

range of analysis, the fluid loading effect is important while the curvature effect of the cylinder can be neglected.

The results associated with the cylinder with stiffeners spaced at 0.38 m are presented first. The corresponding attenuation constant is presented in Fig. 3. It can be observed that there are two stop bands within the analyzed frequency range. The power transfer coefficients that are computed from the attenuation constant of the PS theory are presented in Fig. 4. The periodic characteristics are accounted in the values of the power transfer coefficients which are incorporated in the computation of the joint matrix in the EFEA formulation. The power

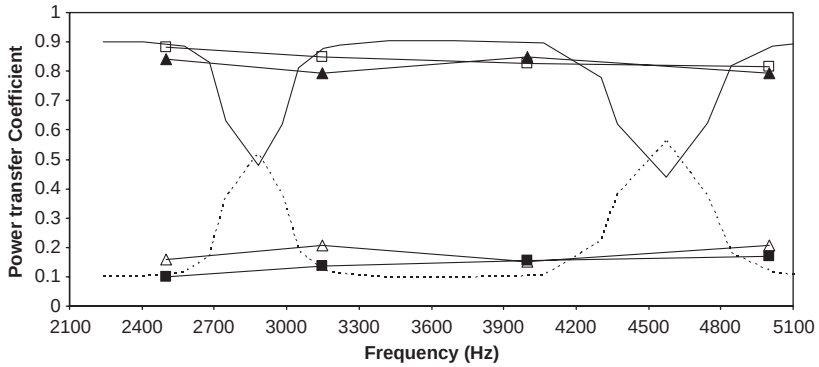

Fig. 4. Power transmission coefficients from PS theory: ——, transmission (EFEA-PS); - - - - , reflection (EFEA-PS); —▲—, transmission(EFEA-PS, center frequency); –△– , reflection(EFEA-PS, center frequency); —■—, transmission (EFEA-PS, center frequency); –□–, reflection (EFEA-PS, center frequency).

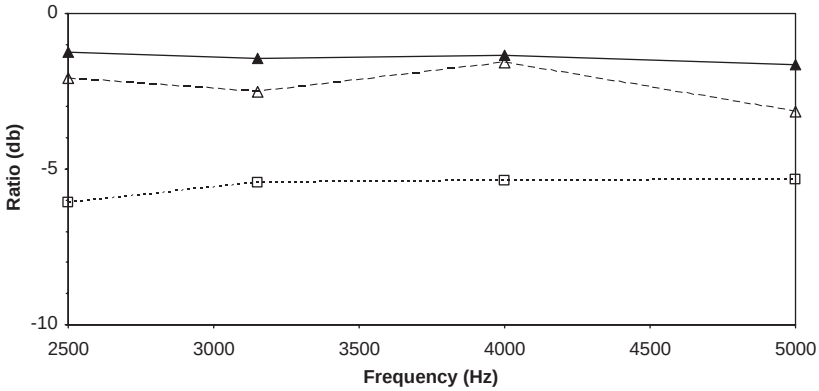

Fig. 5. Energy ratio between periodic unit 2/periodic unit 1: - - △- -, SONAX; —▲—, EFEA-PS; - - □- -, EFEA.

transfer coefficients are computed both at distinct frequencies and also as averaged values for each one-third octave band. The EFEA computations are performed both at the center frequencies of the one-third octave bands and at distinct frequencies. The EFEA analyses are performed at distinct frequencies in order to demonstrate better the stop bands in the EFEA formulation. Typically, in high-frequency computations analyses are performed in one-third octave bands. FEA analyses are performed at ~6 Hz frequency intervals throughout the entire frequency range of analysis. Energy variables are computed from the displacement results of the FEA analyses and they are also frequency averaged over each one-third octave in order to be compared properly with the EFEA frequency averaged results. The ratio computed by both methods between the energy stored in a receiving unit over the energy stored in the unit where the excitation is applied is presented in Figs. 5–8 for units 2,3, 8 and 9, respectively. In this manner results are presented both for units close to the excitation and for units far from the excitation. Good correlation is observed between the FEA analysis and the EFEA-PS method. Results computed by the EFEA method with power transfer coefficients that account for the stiffener and the fluid loading effects but not

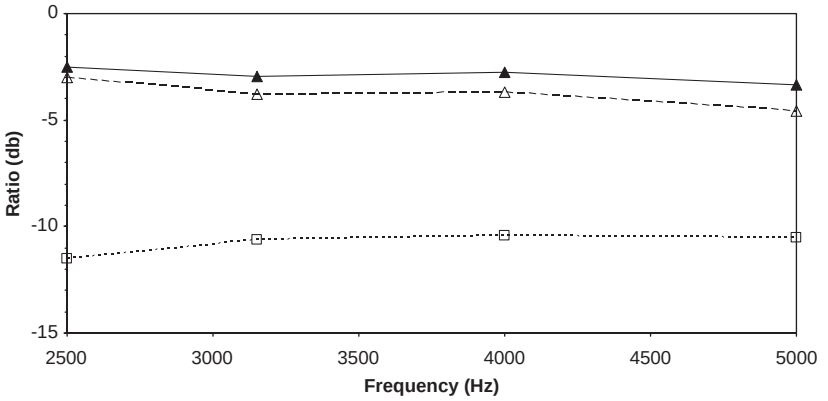

Fig. 6. Energy ratio between periodic unit 3/periodic unit 1: - - △- -, SONAX; —▲—, EFEA-PS; - - □- -, EFEA.

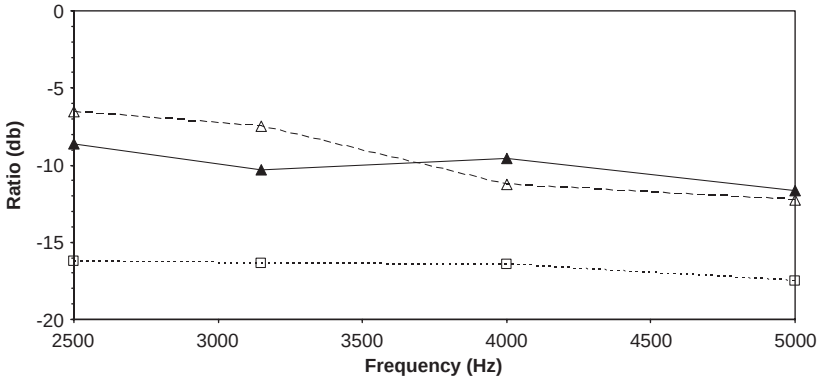

Fig. 7. Energy ratio between periodic unit 8/periodic unit 1: - - △- -, SONAX; —▲—, EFEA-PS; - - □- -, EFEA.

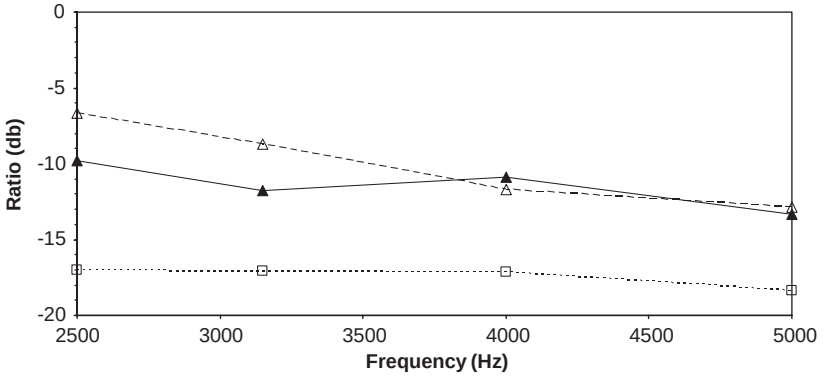

Fig. 8. Energy ratio between periodic unit 9/periodic unit 1: - - △- -, SONAX; —▲—, EFEA-PS; - - □- -, EFEA.

account for the periodicity of the structure are also presented. As it can be observed a considerably lesser amount of power is transferred to the receiving units if the periodic effects are not taken into account. It can be observed that the EFEA-PS method captures well both the fluid-loading effect and the periodic characteristics. For units 8 and 9 results computed by the FEA and the EFEA-PS at individual frequencies are presented in Figs. 9 and 10. In this manner it can be observed that the stop band regions are captured in the EFEA-PS results. In order to further investigate the validity of the EFEA-PS method, the location of the excitation is moved from unit 1 to unit 3. Analyses are repeated by the SONAX and the hybrid EFEA-PS method. Frequency averaged results over a one-third octave band for Sections 9 and 10 are presented in Figs. 11 and 12. The results computed by FEA and the EFEA-PS correlate well, while the EFEA results that do not include the periodic effects predict a considerably lower power transfer. Results from the FEA and the EFEA-PS computations are presented for the periodic units 9 and 10 for distinct frequencies in Figs. 13 and 14 in order to demonstrate how the stop bands information is captured by the EFEA-PS solution.

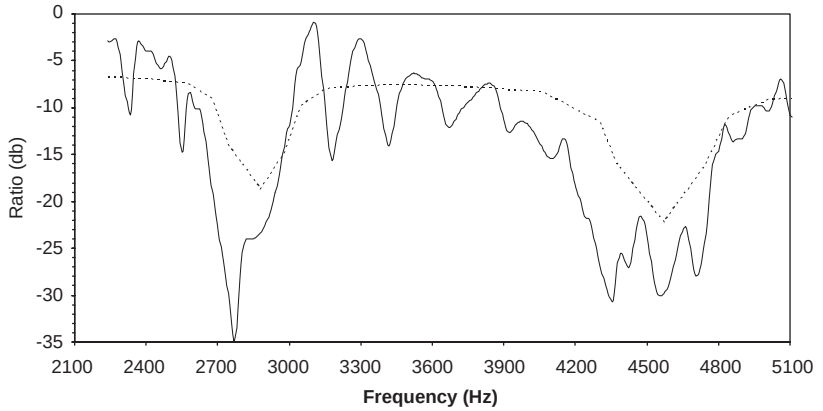

Fig. 9. Energy ratio between periodic unit 8/periodic unit 1: ——, SONAX; - - - - , EFEA-PS.

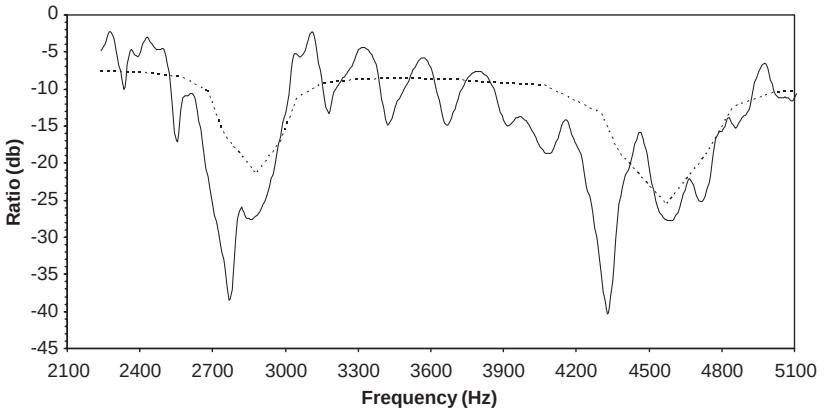

Fig. 10. Energy ratio between periodic unit 9/periodic unit 1: ——, SONAX; - - - - , EFEA-PS.

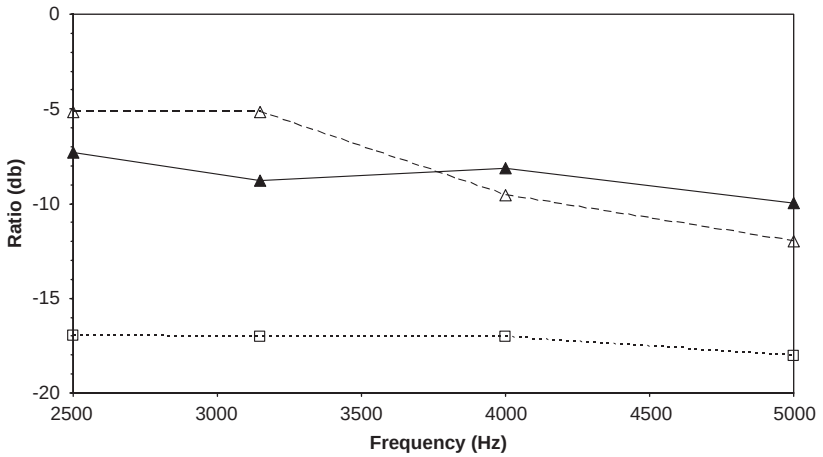

Fig. 11. Energy ratio between periodic unit 9/periodic unit 3: - - △- -, SONAX; —▲—, EFEA-PS; - - □- -, EFEA.

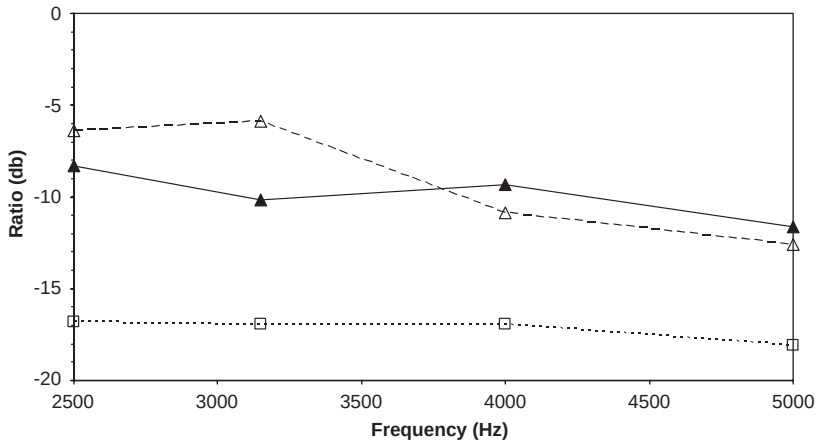

Fig. 12. Energy ratio between periodic unit 10/periodic unit 3: - - △- -, SONAX; —▲—, EFEA-PS; - - □- -, EFEA.

Finally, results are presented for the cylindrical structure with stiffeners placed 1 m apart. The flexural wave attenuation constant is presented in Fig. 15. Four stop band ranges can be observed in this case due to different spacing between the stiffeners. Excitation is applied on unit 1 and results for the two periodic units 9 and 10, which are farthest away from the excitation, are presented in Figs. 16 and 17. The same number of stop-bands is observed between the two solutions, and the stop bands occur in similar frequency ranges between the two methods.

5. Conclusions

A hybrid method that combines the EFEA and the Periodic Structure theory for analyzing the high-frequency vibration of a fluid-loaded cylindrical shell with periodic circumferential stiffeners

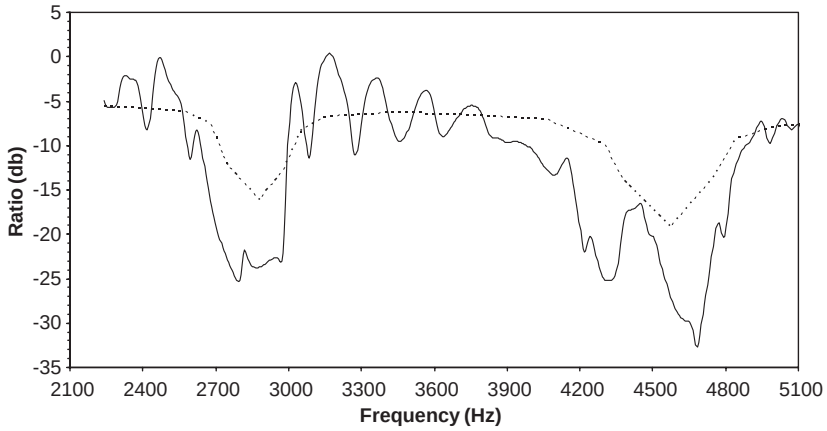

Fig. 13. Energy ratio between periodic unit 9/periodic unit 3: ——, SONAX; - - - - , EFEA-PS.

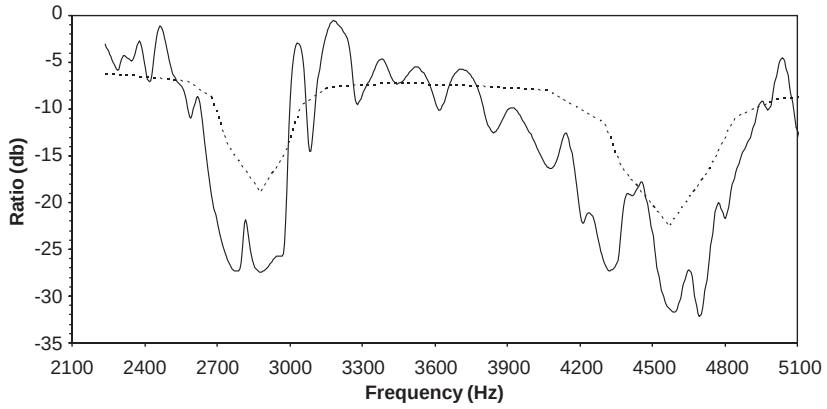

Fig. 14. Energy ratio between periodic unit 10/periodic unit 3: ——, SONAX; - - - - , EFEA-PS.

under an axisymmetric excitation is presented. The added mass and the radiation effects are included in the derivation of the EFEA formulation. The fluid loading effect and the effect from the periodic stiffeners are accounted in the derivation of the power transfer coefficients and in the derivation of the joint matrices in the EFEA. The new hybrid formulation and its implementation is validated by comparing EFEA results to solutions obtained by very dense conventional FEA models. Cylindrical shells with periodic circumferential stiffeners are analyzed. The energy ratio between receiving periodic units and the excited unit are computed by both FEA and EFEA-PS methods. Results from the EFEA solution with power transfer coefficients that do not account for the periodicity effects are also presented. Overall, good correlation is observed between the axisymmetric FEA results and the EFEA-PS solution. The values for the predicted power transfer between receiving periodic units and the excited one are similar between the two methods. The same number of stop bands and at similar frequencies are also predicted by the two methods.

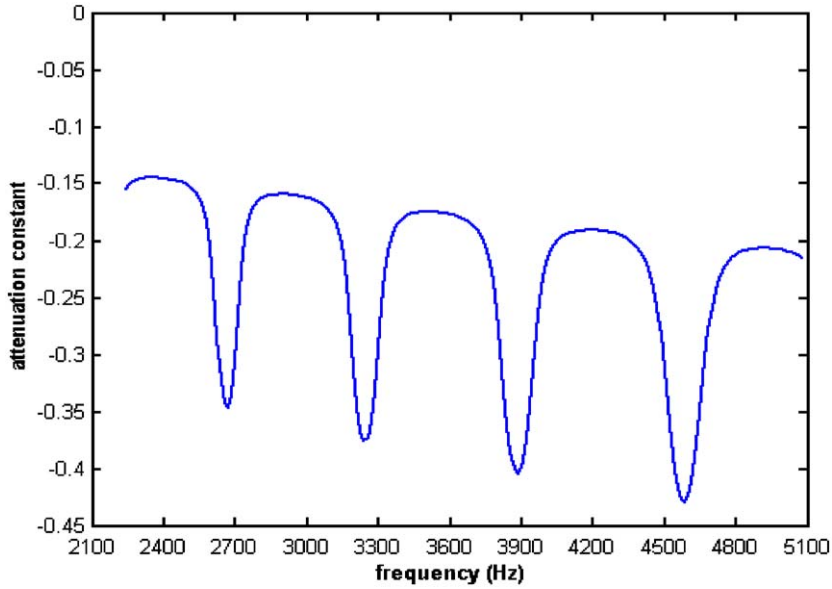

Fig. 15. The flexural wave attenuation constant of the circumferentially stiffened cylindrical shell with stiffeners spaced at 1.0 m.

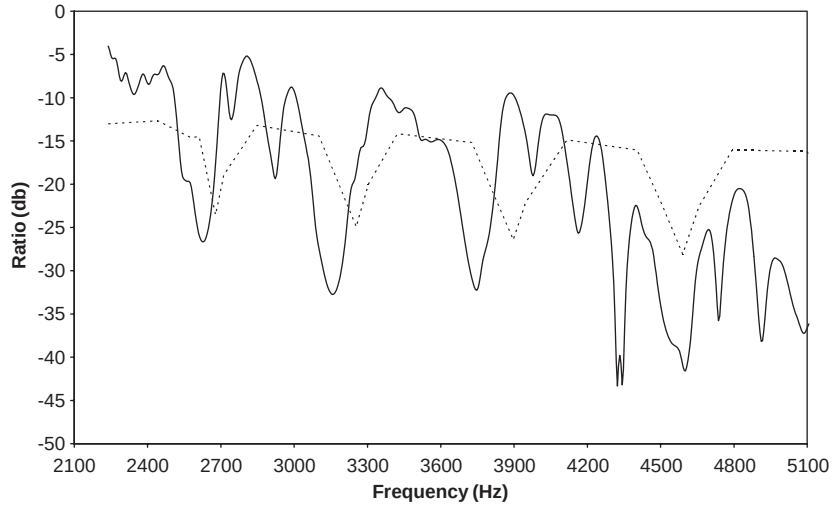

Fig. 16. Energy ratio between periodic unit 9/periodic unit 1: ——, SONAX; - - - - , EFEA-PS.

Finally, the difference between the EFEA-PS and the EFEA results that do not account for periodicity in the derivation of the power transfer coefficients demonstrates the importance of including the periodic effects in the EFEA computations.

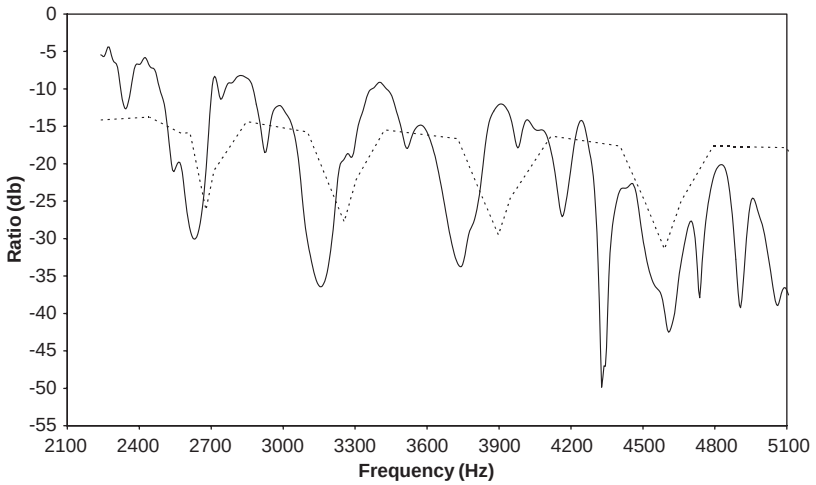

Fig. 17. Energy ratio between periodic unit 10/periodic unit 1: ——, SONAX; - - - - , EFEA-PS.

Acknowledgements

The present research in this paper was supported by the office of Naval Research, Code 334, under Contract Number N00014-00-0382.

Appendix A. Definition of entries in structural property matrix

The detail expressions for functions f_i and g_i $(i = 1, 3)$ are

$$f_1(\lambda_s) = -\frac{E_c h}{(1-v^2)}\left(\lambda_s\psi(\lambda_s) + \frac{v}{R}\right) + \tfrac{1}{2}\rho_0 A\omega^2(-\psi(\lambda_s) + b\lambda_s),$$

$$f_2(\lambda_s) = -\frac{E_c h^3}{12(1-v^2)}(-\lambda_s^3) + \frac{1}{2}\left(\frac{E_0 A}{R^2} - \rho_0 A\omega^2\right),$$

$$f_3(\lambda_s) = \frac{E_c h^3}{12(1-v^2)}(-\lambda_s^2) + \frac{1}{2}\left(-\frac{E_0 I_{zz}}{R^2}\lambda_s + \rho_0\omega^2(I_p\lambda_s - Ab\psi(\lambda_s))\right),$$

$$g_1(\lambda_s) = \frac{E_c h}{(1-v^2)}\left(\lambda_s\psi(\lambda_s) + \frac{v}{R}\right) + \tfrac{1}{2}\rho_0 A\omega^2(-\psi(\lambda_s) + b\lambda_s),$$

$$g_2(\lambda_s) = -\frac{E_c h^3}{12(1-v^2)}\lambda_s^3 + \frac{1}{2}\left(\frac{E_0 A}{R^2} - \rho_0 A\omega^2\right),$$

$$g_3(\lambda_s) = \frac{E_c h^3}{12(1-v^2)}\lambda_s^2 + \frac{1}{2}\left(-\frac{E_0 I_{zz}}{R^2}\lambda_s + \rho_0\omega^2(I_p\lambda_s - Ab\psi(\lambda_s))\right),$$

where $s = 1, 6$.

All the terms in the above equations have been defined within Section 3.

References

[1] N. Vlahopoulos, L.O. Garza-Rios, C. Mollo, Numerical implementation, validation, and marine applications of an energy finite element formulation, *Journal of Ship Research* 43 (1999) 143–156.

[2] W. Zhang, A. Wang, N. Vlahopoulos, K. Wu, High frequency vibration analysis of thin elastic plates under heavy fluid loading by an energy finite element formulation, *Journal of Sound and Vibration* 263 (2003) 21–46.

[3] W. Zhang, A. Wang, N. Vlahopoulos, An alternative energy finite element formulation based on incoherent orthogonal waves and its validation for marine structures, *Finite Elements in Analysis and Design* 38 (2002) 1095–1113.

[4] G. SenGupta, Vibration of periodic structures, *Shock and Vibration Digest* 112 (1980) 17–31.

[5] D.J. Mead, Wave propagation in continuous periodic structures: research, contributions from Southampton 1964–1995, *Journal of Sound and Vibration* 190 (1996) 495–524.

[6] R. Lyon, *Statistical Energy Analysis of Dynamical Systems: Theory and Application*, The MIT Press, Cambridge, MA, 1975.

[7] J. Woodhouse, An approach to the theoretical background of statistical energy analysis applied to structural vibration, *Journal of the Acoustical Society of America* 69 (1981) 1695–1709.

[8] D.G. Crighton, The 1988 Rayleigh Medal Lecture: fluid loading—the interaction between sound and vibration, *Journal of Sound and Vibration* 133 (1989) 1–27.

[9] A.J. Keane, W.G. Price, Statistical energy analysis of periodic structures, *Proceedings of Royal Society of London A* 423 (1989) 331–360.

[10] R.S. Langley, J.R.D. Smith, F.J. Fahy, Statistical energy analysis of periodically stiffener damped plate structures, *Journal of Sound and Vibration* 208 (1997) 407–426.

[11] R.S. Langley, The frequency band-averaged wave transmission coefficient of a periodic structure, *Journal of the Acoustical Society of America* 100 (1996) 304–311.

[12] O.M. Bouthier, R.J. Bernhard, Models of space-averaged energetics of plates, *AIAA Journal* 30 (1992) 34–44.

[13] P. Cho, Energy Flow Analysis of Coupled Structures, PhD Dissertation, Mechanical Engineering Department, Purdue University, Lafayette, IN, 1993.

[14] J.E. Huff Jr., R.J. Bernhard, Prediction of high frequency vibrations in coupled plates using energy finite elements, *Proceedings Inter-Noise 95*, Newport Beach, CA, USA, 1995, pp. 1221–1126.

[15] D.J. Nefske, S.H. Sung, Power flow finite element analysis of dynamic systems: basic theory and applications to beams, *Journal of Vibration, Acoustics, Stress and Reliability* 220 (1999) 135–154.

[16] R.J. Bernhard, J.E. Huff Jr., Structural-acoustic design at high frequency using the energy finite element method, *Journal of Vibration and Acoustics* 121 (1999) 295–301.

[17] D.J. Mead, N.S. Bardell, Free vibration on a thin cylindrical shell with discrete axial stiffeners, *Journal of Sound and Vibration* 111 (1986) 229–250.

[18] D.J. Mead, N.S. Bardell, Free vibration on a thin cylindrical shell with periodic circumferential stiffeners, *Journal of Sound and Vibration* 115 (1987) 499–520.

[19] N. Vlahopoulos, Xi Zhao, T. Allen, An approach for evaluating power transfer coefficients for spot-welded joints in an energy finite element formulation, *Journal of Sound and Vibration* 220 (1999) 135–154.

[20] D.E. Beskos, J.B. Oates, Dynamic analysis of ring-stiffened circular cylindrical shells, *Journal of Sound and Vibration* 75 (1981) 1–15.

[21] D.M. Photiadis, Wave mixing effects on a periodically ribbed cylindrical shell, *Journal of Vibration and Acoustics* 118 (1996) 100–106.

[22] T. Bazow, *SONAX User's Manual*, Naval Research Laboratory, Washington DC, 1997.

[23] A.J. Keane, W.G. Price, On the vibrations of mono-coupled periodic and near-periodic structures, *Journal of Sound and Vibration* 128 (1989) 423–450.

[24] H. Jamshidiat, G. SenGupta, Dynamics of periodic structures interacting with an enclosed fluid medium, *Journal of Sound and Vibration* 148 (1991) 103–115.

[25] F.G. Leppington, E.G. Broadbent, F.R.S., K.H. Heron, The acoustic radiation efficiency of rectangular panels, *Proceedings of the Royal Society of London A* 382 (1982) 245–271.

[26] G. Maidanik, Response of ribbed panels to reverberant acoustic fields, *Journal of the Acoustical Society of America* 34 (1962) 809–826.
[27] L. Cremer, M. Heckl, E.E. Ungar, *Structure-Borne Sound*, Springer, Berlin, 1973.
[28] H. Kraus, *Thin Elastic Shells*, Wiley, New York, 1967.
[29] D.M. Photiadis, Fluid loaded structures with one dimension disorder, *Applied Mechanics Review* 49 (1996) 100–125.
[30] R.S. Langley, K.H. Heron, Elastic wave transmission through plate/beam junctions, *Journal of Sound and Vibration* 143 (1990) 214–253.